Lab on a Chip

PAPER

View Article Online
View Journal | View Issue

Cite this: *Lab Chip*, 2025, **25**, 546

Repackable microfluidic molecularly imprinted solid-phase extraction coupled with mass spectrometry (μMISPE-MS) for rapid analysis of mycotoxin in agri-foods: an example of zearalenone

Marti Z. Hua,[a] Jinxin Liu,[a] Tianqi Li,[b] David R. McMullin,[b] Yaxi Hu*[b] and Xiaonan Lu *[a]

Mycotoxins are detectable in 60–80% of food crops, posing significant threats to human health and food security, and causing substantial economic losses. Most mitigation approaches focus on detecting mycotoxins with standard methods based on liquid chromatography coupled with mass spectrometry (LC-MS). Typical MS methods require extensive sample preparation and clean-up due to the matrix effect, followed by time-consuming LC separation, complicating the analysis process and limiting analytical throughput. This study reports the development of a repackable microfluidic molecularly imprinted solid-phase extraction coupled with mass spectrometry (μMISPE-MS) method for rapid detection of zearalenone in agri-food samples. Silica microspheres coated with molecularly imprinted polymers were synthesized as the sorbent for analyte enrichment and sample clean-up. A cost-effective microfluidic chip was designed and fabricated as the μMISPE platform with fully automated operation, including on-line microcolumn packing and unpacking. With optimized solvent conditions and on-chip μMISPE protocol, the entire analytical process from sample to answer was completed within 15 min and achieved high recoveries (71–94%) for corn and rice samples at residue levels of 0.05–0.5 ppm (within Canadian regulatory limits of 0.2–10 ppm). This μMISPE-MS method provides a promising tool for improving mycotoxin monitoring in agri-food systems and is generalizable to other rapid analyses of targeted chemicals in complex matrices.

Received 12th September 2024,
Accepted 6th January 2025

DOI: 10.1039/d4lc00760c

rsc.li/loc

1. Introduction

The agriculture and agri-food sectors play a vital role in strengthening food security and are a major contributor to the Canadian economy. However, it faces many challenges in providing safe and nutritious food products both domestically and globally.[1] Among these challenges, mycotoxin contamination is particularly concerning due to its high prevalence, as these chemicals produced by certain moulds are detectable in up to 60–80% of food crops and as much as 80% of animal feeds globally.[2] Consuming contaminated food or feed can pose serious health threats to humans and livestock, such as cancers, compromised immune systems, and reproduction issues.[3] Many mycotoxins are relatively stable during general food and feed processing procedures. To effectively mitigate the contamination of mycotoxin and ensure food safety, accurate determination of their residue levels in agri-foods is indispensable.

Currently, the standard methods for analyzing mycotoxins in agri-foods rely on liquid chromatography coupled with mass spectrometry (LC-MS) or with other detectors (*e.g.*, fluorescence detector).[4] LC-MS is undoubtedly sensitive and accurate, fitting the analytical needs for routine analysis of single or multiple mycotoxins in various sample types for regulatory purposes. However, the limitations of LC-MS become more evident when there is a need for higher throughput and lower costs without compromising the analytical reliability. For example, the mandatory sample clean-up and enrichment steps, from classic multi-step partitioning to more recent QuEChERS (Quick, Easy, Cheap, Effective, Rugged, and Safe) method, are often time-consuming and labour-intensive. These steps also require costly consumables and generate significant amounts of hazardous chemical waste though only microlitres of sample extracts are injected into the LC-MS system eventually.[5,6] In addition to MS, antibody-based methods, particularly the

[a] *Department of Food Science and Agricultural Chemistry, McGill University Macdonald Campus, Sainte-Anne-de-Bellevue, Quebec, H9X 3V9, Canada. E-mail: xiaonan.lu@mcgill.ca*
[b] *Department of Chemistry, Carleton University, Ottawa, Ontario, K1S 5B6, Canada. E-mail: yaxihu@cunet.carleton.ca*

enzyme-linked immunosorbent assay (ELISA), are sometimes recognized as (semi-)quantitative methods for single mycotoxin screening in compliance with regulations, but the performance is highly dependent on the quality of manufacturer, storage/transportation conditions, and the operation skills of end-users. As a result, MS-based methods remain the preferred practice for quantification of mycotoxins in agri-food samples, which necessitates research and engineering efforts on more rapid, low-cost and user-friendly procedures for sample extraction, clean-up, enrichment, and separation prior to MS analysis.

A few directions have been explored by researchers and industrial professionals, including but not limited to the dilute-and-shoot approach and various forms of solid-phase extraction (SPE).[7] The dilute-and-shoot technique originally refers to diluting a sample with a suitable solvent for direct injection into the detection system (*e.g.*, MS, LC-MS), which is commonly used for simpler sample matrices (*e.g.*, biological fluids, filtered beverages).[6] In recent years, the dilute-and-shoot approach has been explored for simultaneous quantification of hundred to >1200 chemical contaminants of different classes in complex food and feed matrices.[8–10] For most agri-food samples, although minimal extraction or partitioning is mandatory, dilute-and-shoot is still time- and cost-efficient than conventional methods. However, this approach often results in irreproducible matrix effects and necessitates a well-developed chromatography method coupled to a mass spectrometer due to the complexity of agri-food matrices.[6,9] On the other hand, techniques derived from SPE continue to be optimized to minimize material and labour costs, particularly through the development of miniaturized apparatus and fully automated device. As a good example, an on-line SPE system has been commercialized for sample clean-up and analyte enrichment with the option of being integrated as a module into an LC-MS system.[11] When analyzing a single analyte or a group of structurally similar compounds (*e.g.*, a single mycotoxin or its derivatives), molecularly imprinted SPE (MISPE) has demonstrated unique advantages over non-specific SPE sorbents (*e.g.*, C_{18}, graphitized carbon black) by offering high selectivity and adsorption capacity similar to that of an immunoaffinity column. Nonetheless, concerns about the reuse of SPE columns, such as the need for column regeneration and the risk of carryover or contamination, may limit the popularity of these techniques.[12] Detailed investigation of the carryover phenomenon and optimization of the regeneration procedure needs to be performed to further reduce the costs of materials or consumables and enhance the sustainability of the extraction methods.

A microfluidic chip, often refer to as a "lab-on-a-chip", is a miniaturized device with specially designed patterns that allow the manipulation of fluids at the microscale. This platform originated from the concept of the micro total analysis system in the 1990s and thrived since the introduction of polydimethylsiloxane (PDMS) and well-established fabrication protocols.[13] As microfluidic devices can integrate one or more conventional bench experiments with high automation potential, various functional designs and applications have been reported in many research fields, such as diagnostic sensors and organ-on-chips for drug development.[14,15] Over the past 15 years, the application of microfluidic techniques in food safety control has drawn increasing interest, with many studies reporting the development of analytical devices made of PDMS and porous or nonwoven materials (mainly paper-based devices) for detecting food hazards.[15–17] Despite being a promising platform for detecting chemical hazards in agri-food, PDMS-based microfluidic devices face several challenges, such as the need for off-chip sample preparation, the lack of specific on-chip sensing agents, and the high cost of disposable PDMS devices, particularly given the demand of agri-food industry for low-cost demand.[18] Applications of molecularly imprinted polymers (MIPs) in microfluidic sensors have been more limited, primarily focusing on detecting biomarkers and environment contaminants in simple matrices, such as water and biofluids.[19]

In the current study, we report the development of a repackable microfluidic MISPE coupled with mass spectrometry (μMISPE-MS) to address these challenges and demonstrate the rapid analysis of a mycotoxin zearalenone in agri-foods using the μMISPE-MS method (Fig. 1). A low-cost microfluidic chip was designed and fabricated as the μMISPE platform with full automation controlled by an optimized program. Silica microspheres coated with MIPs were slurry-packed into the main channel for on-chip μMISPE and then unpacked after each test. This design enabled the reuse of the μMISPE chip, simplified the protocol, eliminated the risk of carryover, and significantly reduced material usage and waste compared to conventional MISPE and on-line SPE methods. The cleaned and enriched mycotoxin was eluted and shot directly into the mass spectrometer for immediate data acquisition, bypassing a further separation by LC, and resulting in high recovery and sufficient sensitivity for the quantification of zearalenone in agri-foods at regulated residue levels.

2. Materials and methods

2.1. Materials and instruments

Tetraethyl orthosilicate (TEOS), 3-(trimethoxysilyl)propyl methacrylate (MPS), methacrylic acid, ethylene glycol dimethacrylate (EGDMA), and azobisisobutyronitrile (AIBN) were purchased from Sigma-Aldrich (ON, Canada). Ammonium hydroxide (28–30%, w/w) and glacial acetic acid (HAc) were from Fisher Scientific (ON, Canada). Cyclododecyl 2,4-dihydroxybenzoate (CDHB) was synthesized in-house as previously reported.[20] Zearalenone standard was purchased from Toronto Research Chemicals (ON, Canada). Dow Sylgard 184 Silicone Elastomer Kit was from Ellsworth Adhesives (ON, Canada). Ultrapure water was collected freshly from a water purification system (Millipore Direct-Q, United States). All other solvents were of ACS or HPLC grade from Sigma-

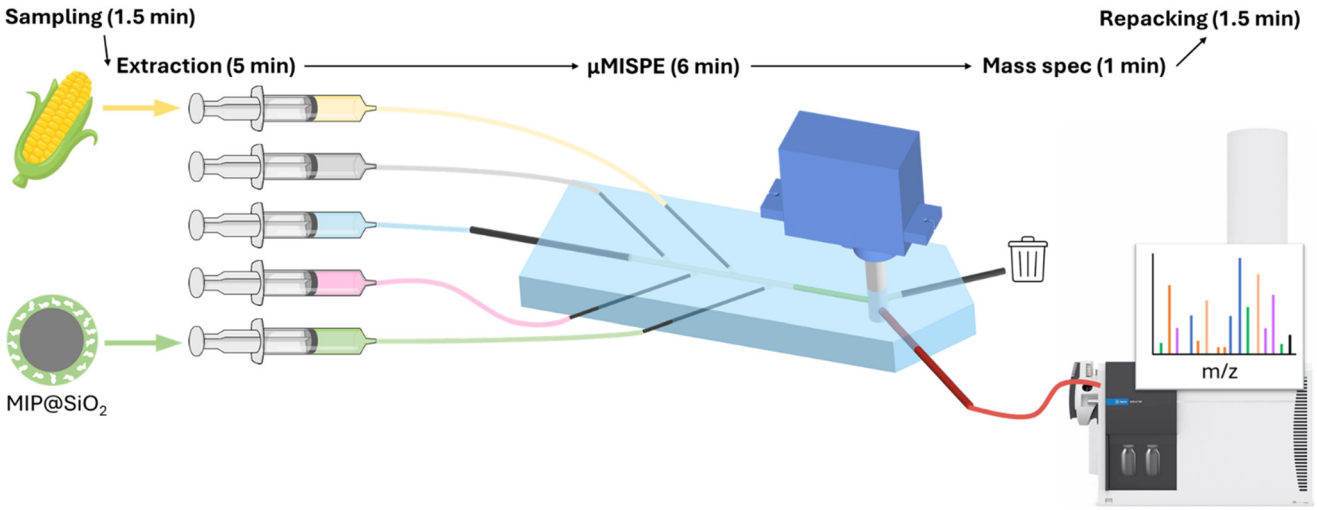

Fig. 1 Schematic illustration of the overall procedures for the rapid analysis of mycotoxin residue in agri-food samples using μMISPE-MS within 15 min.

Aldrich Canada or Fisher Scientific Canada. Agri-food samples were purchased from local markets, and the ones with no detectable zearalenone by HPLC-FLD were used for spiking in the recovery tests. Other raw materials for machining were purchased from McMaster-Carr (United States), Cole-Parmer (QC, Canada), and Agilent (ON, Canada).

Microfluidic syringe pumps were used in the SiO_2 synthesis and for operating the on-chip μMISPE. The Miuzei SG90 Servo Motor, controlled by an ARDUINO A000066 Uno R3 and SunFounder PCA9685 servo driver, was used to automate the valve on the microfluidic chip. A Yakamoz micro-drill was used for micromachining the valve. A Waters Breeze HPLC-FLD was used for accurate quantification of zearalenone in the adsorption tests and MISPE solvent optimization with the condition as previously reported.[20] MS spectra were acquired with an Agilent 6230B time-of-flight mass spectrometer (Agilent Technologies, Palo Alto, CA, USA) equipped with an electrospray ionization (ESI) source that was directly connected to the outlet of microfluidic chip for sample injection. Transmission electron microscopy (TEM) images were acquired using a Thermo Scientific Talos F200X G2 (S)TEM system hosted at the Facility for Electron Microscopy Research at McGill University.

2.2. Synthesis and characterization of MIPs

Silica microspheres were synthesized using a modified Stöber method.[21] Briefly, 68 mg of KCl in 27 mL of H_2O, 260 mL of ethanol and 36 mL of ammonium hydroxide were mixed at room temperature (~20 °C). Then, 8 mL of TEOS in 133.4 mL of ethanol was added at 800 μL min^{-1}, followed by additional magnetic stirring for 16 h. The synthesized particles were collected by centrifugation, washed three times with ethanol, and vacuum dried at room temperature overnight.

The surface of SiO_2 microspheres was modified with vinyl groups following a previously reported protocol.[22] Briefly, 1 g of SiO_2 microspheres were resuspended in 250 mL of ethanol : H_2O (4 : 1, v/v) by sonication. Then, 7.5 mL of ammonium hydroxide and 4 mL of MPS were added with magnetic stirring at 65 °C for 24 h. The modified particles were collected by centrifugation, washed three times with ethanol, and vacuum dried at room temperature overnight.

For the synthesis of MIPs, 0.05 mmol of CDHB and 0.2 mmol of methacrylic acid were dissolved in 45 mL of acetonitrile and incubated for 30 min, followed by adding 100 mg of vinyl–SiO_2 suspended in 5 mL of acetonitrile. Then, 1 mmol of EGDMA and 20 mg of AIBN were dissolved into the mixture, followed by purging with nitrogen gas for 5 min. The mixture was heated at 65 °C with magnetic stirring for 24 h to allow for polymerization. The resulting particles were collected by centrifugation, washed with 10% acetic acid in methanol to remove the template, and rinsed with pure methanol to remove acetic acid residue. The resulting MIPs were vacuum-dried at 60 °C for 6 h. Non-imprinted polymers (NIPs) were prepared following the same procedure in the absence of the template CDHB. CDHB was selected as a dummy template instead of using the target mycotoxin zearalenone due to their structural similarity and the consideration in template bleeding and material availability.[20,23]

In the static adsorption test, 5 mg of MIPs or NIPs was mixed with 1 mL of zearalenone standard solution (40% in acetonitrile) at different concentrations (10, 25, 50, 75 and 100 μg L^{-1}) for 60 min with continuous rotary shaking. The mixtures were then centrifuged, and the remaining concentration of zearalenone in the supernatant was determined by HPLC-FLD. In the dynamic adsorption test, MIPs or NIPs were mixed with zearalenone solution (50 μg L^{-1}) at the ratio of 5 mg to 1 mL with continuous rotary shaking. At each time point (*i.e.*, at 2, 5, 10, 20, 30, and 60 min), a 1 mL aliquot was collected, immediately centrifuged, and the remaining concentration of zearalenone in the supernatant was determined by HPLC-FLD. The adsorption (Q) was calculated as $Q = (c_0 - c) \times V/m$, where c_0 is the initial

concentration, c is the concentration in the supernatant, V is the volume of the zearalenone solution, and m is the mass of MIPs or NIPs.

Transmission electron microscopy images were acquired to examine the size, shape and MIP coating of the microsphere.

2.3. Fabrication of the microfluidic chip

The main body of the microfluidic chip was fabricated *via* a two-step cast moulding. Briefly, the PDMS base and curing agent were mixed at the ratio of 9 : 1 by weight and degassed under vacuum. The mixture was poured into a plastic petri dish to ~40% of its depth and placed in a vacuum desiccator for ~24 h at room temperature. Then, straight metallic wires (plastic coating removed) of different diameters were cut into the desired lengths and carefully placed on the semi-solidified PDMS as the mould for the channels. Another layer of degassed PDMS mixture was added to fill ~90% of the dish which was then left in vacuum desiccator for ~48 h. The cured PDMS was cut along the outline of the design, and the wires were removed to create the channels. A polytetrafluoroethylene (PTFE) rod was cut, drilled, polished, and installed in the punched hole of the PDMS chip to function as the micro-valve. The top of the rod was either connected to a servo for programmed control or fitted with a wire for manual operation. A stainless-steel frit and a PEEK tubing were installed at the outlet for connecting to the ESI source of the MS system. All inlets and the waste outlet were connected *via* stainless-steel needles.

2.4. Optimization of μMISPE conditions

Seven different solvent combinations were tested for MISPE using the zearalenone standard solution, and the operations in μMISPE were further optimized for full automation. The recovery was determined by HPLC-FLD. Correspondingly, improvements in chip fabrication were made (*e.g.*, adjusting part dimensions, the volume of solvent, and flow rate) to meet the requirement of μMISPE.

2.5. Analysis of agri-food samples

Agri-food samples were homogenized for 1 min, and 10 g of sample was mixed with 25 mL of 90% acetonitrile(aq) in a 50 mL centrifuge tube and sonicated for 5 min. After allowing the mixture to settle for 30 s, 1 mL of the liquid extract was drawn into a 3 mL syringe containing 1.5 mL of water passing through a 0.45 μm nylon syringe filter. The syringe was then manually agitated shortly and loaded onto the syringe pump for μMISPE-MS analysis. The ESI-MS settings were as follows: negative mode (ESI−), gas temperature = 325 °C, flow rate of drying gas = 10 L min^{-1}, nebulizer pressure = 20 psi, sheath gas temperature = 400 °C, flow rate of sheath gas = 12 L min^{-1}, and VCap = 4000 V. Resulting mass spectra were processed with MZmine 4.2ver.

3. Results and discussion

3.1. Synthesis and characterization of MIPs

The molecular imprinting technique has been developed for decades with proven potential in replacing antibodies in many applications in chemical analysis.[24,25] Compared with biomolecule-based recognizing agents (*e.g.*, antibodies, aptamers), molecularly imprinted polymers feature robustness and flexibility in harsh physical and chemical environments with much lower cost to produce.[24,25] Depending on the specific purpose of an application, the properties of MIPs (*e.g.*, material, form, size) should be carefully considered, and the appropriate synthesis method is then optimized to achieve the desired performance.

In the current study, MIPs with a core–shell structure were synthesized as the sorbent in μMISPE (Fig. 2). The size and shape of the particles were prioritized in the preliminary experiment due to the impact on the internal pressure and sorbent packing for the microfluidic chip. Different from the tightly packed stainless steel microcolumns used in on-line SPE or micro-LC system, a PDMS-chip-based column favours much lower internal pressure to minimize the risk of breakage or leakage at the tubing-chip interface as well as avoid excessive anchor or clamping effect (further discussed later).[26] Particles ranging from tens to hundreds of nanometers resulted in much higher pressure and clogging of filter frits (0.5–10 μm) and even filter paper or membrane (effective pore sizes of 0.2–10 μm) during synthesis trials. Therefore, particles with a diameter of 1.3–1.4 μm (Fig. 2B and C) were selected to balance these issues while maintaining separation efficiency within a relatively short column length. For comparison, particles in a UPLC column are typically 1.6–1.7 μm in diameter. Regarding the shape of the MIPs, monodispersed microspheres with a consistent thickness (~35 nm) of MIPs coating (Fig. 2C and D) would provide a more homogeneous adsorption profile (common strategy in LC columns) and a shorter equilibrium time. In comparison, MIP particles synthesized *via* conventional bulk polymerization were obtained from crushing rigid monoliths and mechanically sieving (*e.g.*, <35 μm or <70 μm with a 200 or 400 mesh sieve), resulting in various size, shape, and surface morphology. SiO_2 was selected as the core to support the MIPs shell given the simplicity of size tuning and dispersity control of this widely used material *via* the well-established Stöber method. Other commonly used supporting materials, such as metal–organic frameworks,[27] would require more complicated synthesis and size/shape control.

Static and dynamic adsorption tests were performed to characterize the MIPs in comparison with the NIPs using the standard solution of zearalenone at the relevant concentrations, accounting for dilution during sample extraction. In the static adsorption test (Fig. 3A), the adsorption capacity of the MIPs was 1.7–3.4 times of that of the NIPs depending on the concentrations, and this difference verified the successful imprinting of the zearalenone-specific binding cavities on the shell of the

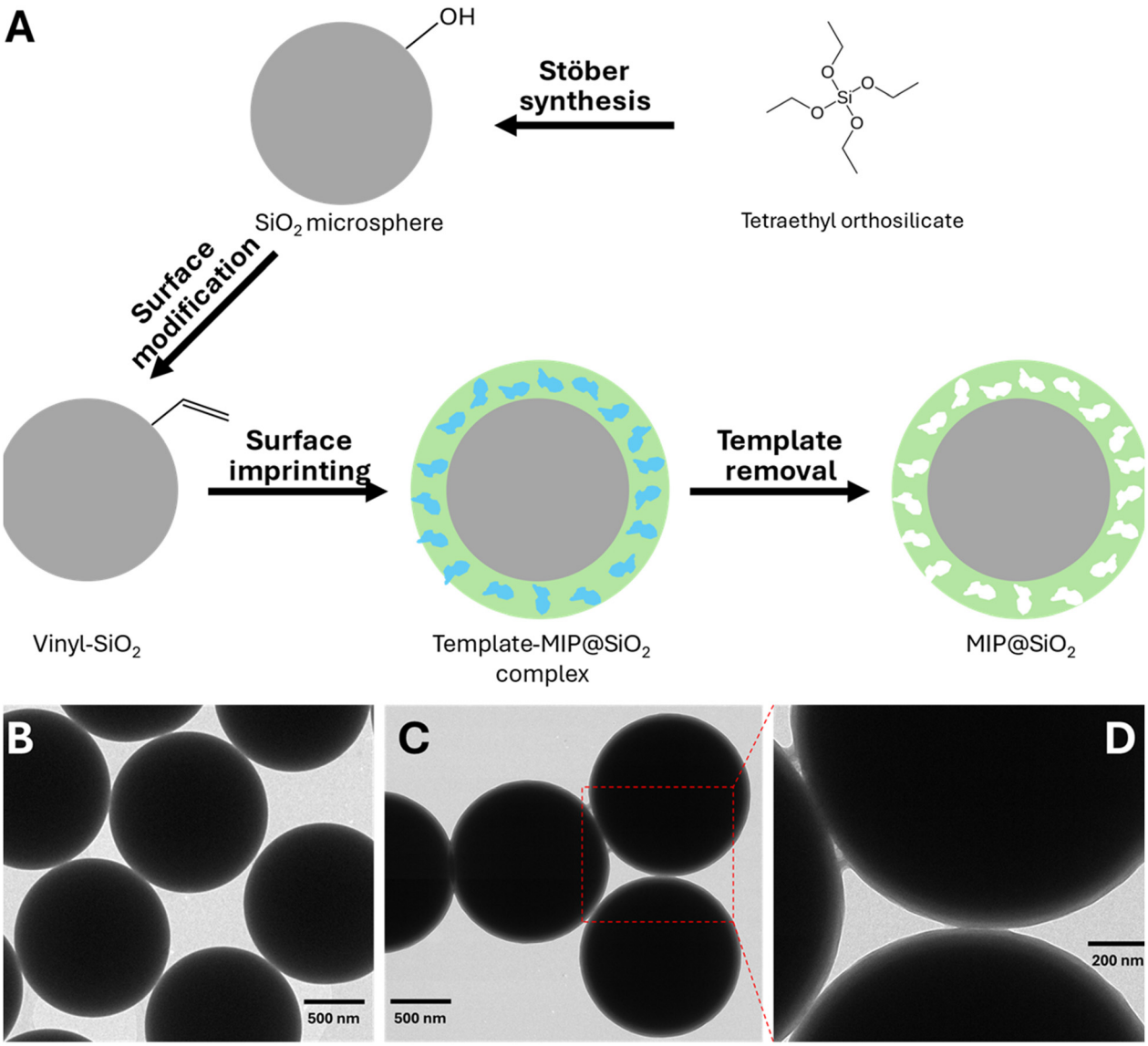

Fig. 2 (A) Scheme of the synthesis of CDHB-templated MIP@SiO_2, and transmission electron microscopy images of (B) SiO_2 microsphere, (C) MIP@SiO_2, and (D) 2.5× zoomed detail of MIP coating.

microspheres. In the dynamic adsorption test (Fig. 3B), the majority of zearalenone was adsorbed in 5 min for MIPs within the time frame of 60 min, and only about 2 min for NIPs, indicating the specificity-related difference in surface morphology and adsorption mechanisms between MIPs and NIPs. Thus, the prepared MIPs were suitable to serve as SPE sorbent and were subjected to further testing for the optimization of MISPE procedures.

3.2. Design and fabrication of the microfluidic chip

3.2.1. Overall design. Ideally, the design of microfluidic chips should align with the specific purpose(s) and analytical requirements for the miniaturization of conventional wet lab operations. In our preliminary experiment, three designs were proposed and briefly tested. The first design aimed to build a fully on-chip version of on-line SPE columns or multi-use SPE cartridges. The typical SPE procedure would include a column regeneration step that required a relatively high percentage of organic acid in pure organic solvent to remove adsorbed impurities and rinse any residual acid, thus prolonging the entire process and subjecting the PDMS chip to greater chemical stress. The second design involved separating the chip into a reusable platform and a replaceable column connected *via* adapters (*e.g.*, mini Luer connectors) to bypass the regeneration step. Although the column could be pre-packed as a consumable, replacing this single-use component still required manual operation or more complicated mechanics for full automation. The third design forms the basis of this study and proposed replacing only the sorbent while retaining all other chip components.

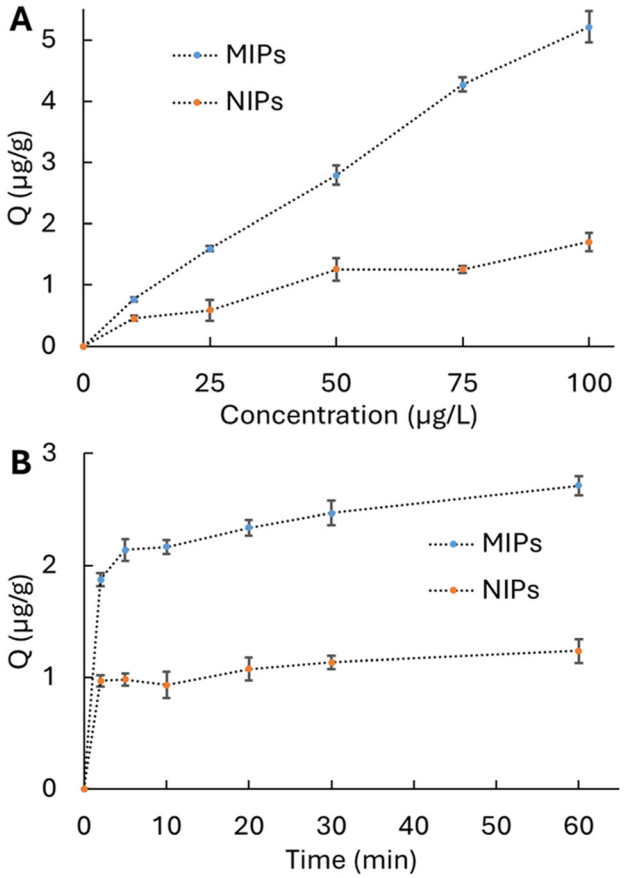

Fig. 3 (A) Static adsorption test of MIPs and NIPs with zearalenone standard solutions (40% acetonitrile) at 10, 25, 50, 75, and 100 μg L^{-1} for 60 min. (B) Dynamic adsorption test of MIPs and NIPs with standard solution at 50 μg L^{-1} with time points at 2, 5, 10, 20, 30, and 60 min (n = 3).

In our design (Fig. 4 and 1), the μMISPE procedure included five steps: 1) packing the μMISPE column by injecting the suspension of sorbents into the main channel *via* the packing inlet; 2) loading the sample extract onto the column *via* the loading inlet; 3) removing interfering sample matrices by injecting solvent *via* the washing inlet; 4) eluting the enriched analyte from the column by injecting eluent *via* the eluting inlet while simultaneously acquiring MS data of the eluate; and 5) unpacking the column and rinsing the channels by injecting solvent *via* the unpacking inlet, flushing waste out of the chip *via* the waste outlet.

This design addresses key challenges, including the on-line packing and unpacking of the μMISPE column, effective manipulation of the eluent and liquid/solid waste, reducing internal pressure at necessary interfaces, and maintaining the potential for full automation of each operation.

3.2.2. Sorbent packing. For on-line column packing, microfluidic slurry-packing was the only option considering the advantages of microfluidic flow and the elasticity of PDMS. Different from packing stainless steel columns or rigid plastic cartridges, the packing and unpacking of a PDMS column were highly affected by the elastomer's softness and flexibility which are largely determined by the ratio of PDMS base to curing agent and the curing temperature. Depending on the shape, size and surface roughness of the sorbent, frit-free approaches had been utilized to initiate the packing (keystone effect in tapered or weir structures) and to lock the sorbent by the clamping-effect and anchor-effect.[26,28–30] However, if on-line unpacking was demanded, a sufficiently wide opening and matching outlet (instead of a tapered end) would be required, and the clamping-effect and anchor-effect would need to be minimized to ensure the release of sorbent with the flow as needed. Moreover, accidental release of sorbent particles into the mass spectrometer should be avoided to reduce the maintenance frequency and potential equipment damage.

Taking these factors into consideration, we designed and fabricated a simple valve vertically installed at the punched hole of the PDMS chip to switch between the two flow directions (Fig. 4). For the packing, loading, washing and eluting steps, the sorbents are held by a stainless-steel frit filter at the outlet connected the MS with the PEEK tubing. For the unpacking step, the valve is switched clockwise, and the used sorbent is flushed out *via* the waste outlet with no blocking (Fig. 4). For the chemical resistant PTFE rod, the surface in contact with the PDMS chip was slightly polished to refine the shape and adjust the roughness, which reduced the friction and the risk of leakage. The path inside the rod (valve) was finalized as a straight tunnel that linked the chip's main channel and MS outlet directly, offset slightly from the central axis of the rod. Since the waste outlet was symmetric to the MS outlet, the rod only needs to be rotated clockwise from the position of the main channel to the waste channel for path switching (Fig. 4), during which the tunnel inside the valve was reversed and the packed column was loosened physically. By optimizing the difference between the diameter of the rod and the punched hole on the PDMS for holding the rod (*i.e.*, friction adjusted), we were able to use a micro servo motor to manipulate the rod for path-switching, which automated this critical manual operation.

3.2.3. Dimension considerations. The dimensions of the chip were determined by balancing the estimated analytical needs with fabrication convenience. Previous studies demonstrated substantially different dimensions of the sorbent holding spaces for packing on-chip columns. For example, a flat glass chamber (~25 mm long and 5 mm wide, with an estimated depth of ~200 μm) had been fabricated to hold ~3 mg of 50 μm C18 particles for pre-MS clean-up.[31] Other studies reported a PDMS channel with a 50 × 70 μm cross-section packed with 3 μm particles for on-chip capillary electrochromatography[28] and a 10 mm PDMS channel with a 245 × 260 μm cross-section packed with 30–40 μm particles for pre-MS μSPE.[29] These designs involved more hazardous operations (*i.e.*, wet etching of glass with hydrofluoric acid) or complicated multi-step cleanroom procedures.

To avoid the complicated and costly procedures, such as photolithography in a cleanroom or plasma treatment, we designed a two-step cast moulding approach to fabricate a

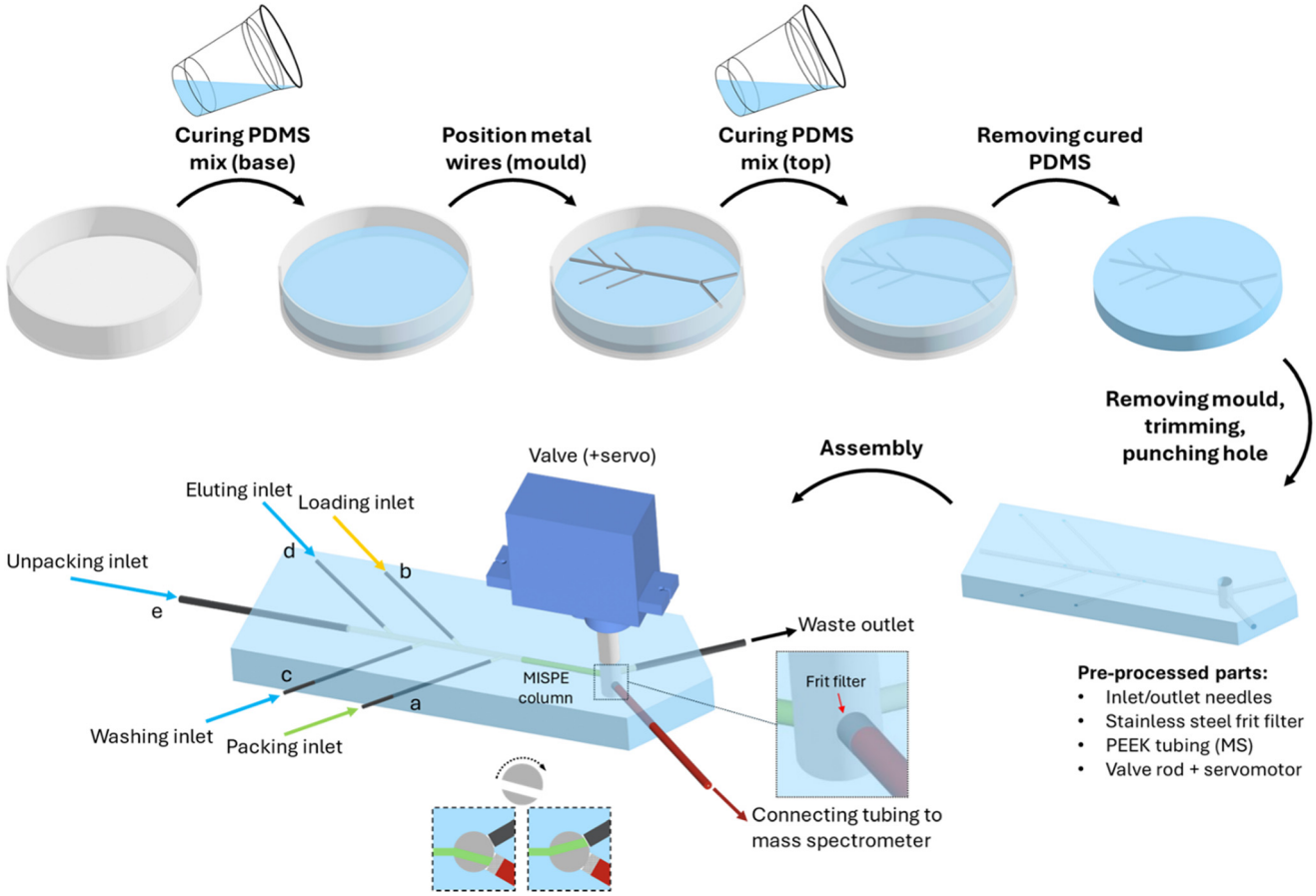

Fig. 4 Fabrication of a PDMS-based microfluidic chip by two-step cast moulding, part processing and assembly, achieving automated operation of on-chip μMISPE for sample clean-up and analyte enrichment prior to MS.

single-piece PDMS chip for hosting MISPE procedures, considering the adsorption performance of MIPs, packing and unpacking issues, and ease of part processing and assembly. As described in the section 2.3 and illustrated in Fig. 4, the dimensions of wires determined the channel shape. The diameters of the wires were 27 gauge (~360 μm) for the main channel in the middle, 21 gauge (~723 μm) for the four side inlet channels, and 18 gauge (~1024 μm) for the two outlet channels. The PTFE rod (1/8″, ~3.175 mm, with a slight reduction for the part in contact with PDMS) was located inside the hole punched by a 3 mm (inside diameter) biopsy punch, and the tunnel within the rod was drilled with a 700 μm drill bit (thus wider than 700 μm). The accurate lengths of the channels were less critical than the selection of compatible inlet/outlet connectors, which further simplified the chip fabrication.

There are a few recommendations for the fabrication steps. First, the container for PDMS curing can be made of hard plastics or metals, both of which are easy to separate from the PDMS slab and can be shaped to match the chip outline, reducing material costs. A customized joining mould produced by 3D printing could further simplify chip trimming and mould reuse. Second, without heating to accelerate the curing process, the PDMS remains sticky after 24 h of room-temperature curing, making this time point ideal for positioning the wires to avoid shifting when adding the top layer of the PDMS mixture. However, if the wires are not correctly positioned on the first attempt, the base layer may be irreversibly damaged. Alternatively, the mould positioning and addition of the top PDMS layer can be completed after the base layer is fully cured. In this case, it is important to double-check and adjust the positions of the wires with forceps carefully, and vibrations or tilting of the container during the curing of the top layer should be avoided. Third, the wires do not have to be extremely straight as the flexibility of PDMS accommodates metal needles and hard tubing insertion. However, straight wires are easier to remove with less risk of damaging the elastomer and leaking at higher internal pressure. Forth. it is also important to ensure that the inside end of wires is smooth necessitating a deburr step after cutting. A similar finishing process can be applied to the sharp inlet needles (or use blunt-tip needles instead) to avoid cracks or misalignment during assembly. Finally, needles with larger outside diameter can achieve a better sealing force between the metal and PDMS, and needles with a larger inside diameter within the same outside diameter (try thin-wall products) may reduce the risk of clogging at the plastic/metal interface during sorbent

injection. It is essential to test the actual outside diameter as it may vary among brands and product lines even with the same gauge number.

3.3. Optimization of μMISPE condition

For MISPE, many factors, very often mutually dependent variables, can impact the effectiveness and efficiency of the extraction process, such as the amount of sorbent, pH, solvent composition and volume, and flow rate.[32] In this study, we focused on optimizing the solvent selection while maintaining most other factors fixed at levels suitable for μMISPE based on preliminary experiments and experience. Seven protocols with the combination of different solvent compositions for loading, washing, and eluting were evaluated to optimize zearalenone recovery (Fig. 5).

In protocol 1, the loading solvent was selected based on the solvent used for sample extraction, while the washing (ACN followed by H_2O) and eluting (acidified ACN) solvents were selected based on solvents in MIP synthesis to minimize non-specific adsorption and remove polar impurities. However, the high percentage of ACN in the loading solvent (followed by pure ACN wash) could reduce the retention of zearalenone when comparing protocols 1 and 2. Therefore, the sample extract was diluted 2.5 times with H_2O to reduce the ACN concentration from 90% to ~36%, which increase the retention of analyte in protocols 3–7. Additionally, 0–70% ACN was tested to reduce analyte loss during the washing step, and a slightly lower recovery with 70% ACN and larger variation with pure H_2O. Lastly, to optimize the eluting solvent, MeOH and acidified MeOH were tested in addition to ACN and acidified ACN, since studies demonstrated strong interfering of MeOH with specific binding mechanisms.[33,34] The solvent combination that provided the highest recovery and reproducibility (96% ± 4%) was 36% ACN for loading, 50% ACN for washing, and MeOH (3% HAc) for eluting (protocol 6).

For on-chip μMISPE, more precise control on the injection of fluids (*i.e.*, sorbent suspension, sample extract, and all other solvents) and the rotation of the microvalve was implemented to harness the potential and overcome the limitation of the microfluidic platform. Several further adjustments were made for practical sample analysis (beyond the simplified steps in section 3.2.1), and all operations were programmed to achieve full automation of μMISPE (Table 1, Fig. 4). First, the packing of the sorbent should, ideally, resemble the typical way of slurry-packing a conventional glass chromatography column, but the internal pressure built up rapidly with a constant flow rate of the MIP suspension as the accumulation of the solid phase. As a result, the downstream end of the microcolumn (the section before the tunnel of the PTFE valve) was susceptible to the anchor or clamping effect, which could hinder the later release of used sorbent. To mitigate this, the suspension injection rate was reduced stepwise. Second, the flow rate in each step impacted the pressure, on-column interaction (efficiency), ionization and signal in the mass spectrometer, the turnaround time of each test, and so on. With the finalized selection of solvents (protocol 6) and parts (needles of 23, 21, and 16 gauge for side inlets a–d, middle inlet e, and waste outlet, respectively; 1/16″ OD frit and tubing for MS outlet), no leakage was observed except for the manual injection test of the MIP suspension which was caused by poor pressure control at the end of packing. Third, a check valve was installed on each syringe for injecting solvents (*i.e.*, *via* inlet c–e, Fig. 4) to prevent backflow. Moreover, during the packing and loading steps, a low flow rate from inlet e was applied, instead of zero, to promote the desired flow direction and minimize undesired backward solvent mixing. Lastly, the rotation of the valve was adjusted by tuning the angular velocity of the servo to reduce the deformation of the PDMS chip (kinetic and static frictions), prevent the frit from moving, and ensure the stableness of the microcolumn.

3.4. μMISPE-MS analysis of agri-food samples

With the optimized protocol, agri-food samples (zearalenone-spiked dried corn kernel and fully processed rice) were analyzed using the developed μMISPE-MS method (Fig. 6D). The ion chromatogram (Fig. 6A) demonstrated the accelerated injection at 100 μL min^{-1} (6–6.5 min, Table 1) of the eluate collected at 30 μL min^{-1} (5–6 min, Table 1) within

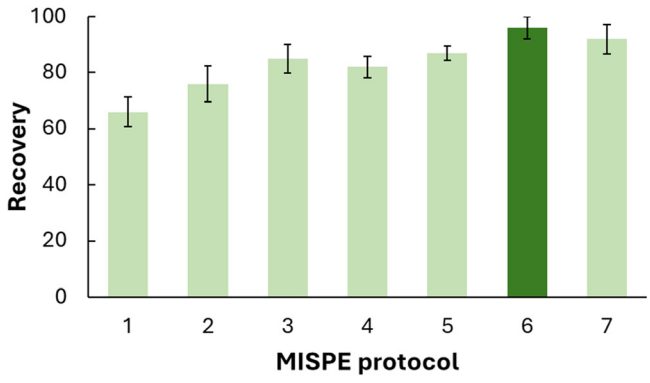

Protocol:	Loading	Washing	Eluting
1	90% ACN	ACN; H_2O	ACN, 2% HAc
2	50% ACN	ACN; H_2O	ACN, 2% HAc
3	36% ACN	H_2O	ACN
4	36% ACN	70% ACN	ACN
5	36% ACN	50% ACN	ACN
6	36% ACN	50% ACN	MeOH, 3% HAc
7	36% ACN	50% ACN	MeOH

Fig. 5 MISPE recoveries of zearalenone with seven different protocols of solvent choices (n = 3).

Table 1 Programed operation of micropump and microvalve for μMISPE

Inlet	Content	0	0.2	0.4	0.6	0.8	1	2	4	5	6	6.5	7	7.5	8	8.5
a	MIP (10% ACN)	200	100	50	20	0							10		0	
b	Sample (36% ACN)	0					30	0						30	0	
c	10% ACN	0						40	0						100	0
d	MeOH, 3% HAc	0								30	100	0		30	0	
e	50% ACN	15		5		30	5	0	30	0		50	300	5	100	0

The unit of time points (top row): min. The unit of flow rates (remaining rows): μL min^{-1}. Valve rotated to waste outlet at 7 min before flow rates were changed. Valve rotated to MS outlet at 8 min after flow rates were changed.

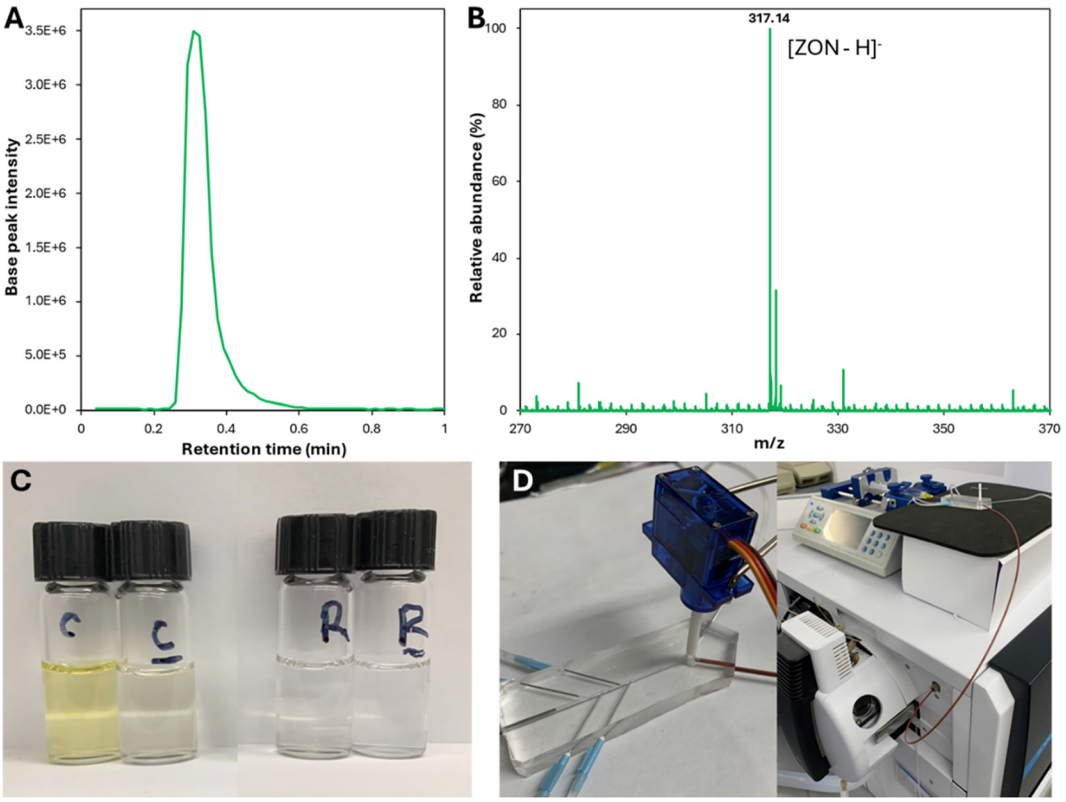

Fig. 6 The (A) base peak ion chromatogram and (B) mass spectrum of zearalenone showing $[ZON–H]^-$ ion at 317.14. Photos of (C) corn and rice samples before and after MISPE and (D) the demonstration of the servo-driven PTFE valve and the connection of μMIPSE to the mass spectrometer.

~0.25 min, and no interfering peaks were observed near the $[ZON–H]^-$ peak in the mass spectrum (Fig. 6B). A balance between the cleanness of the sample and the recovery was achieved, as demonstrated by the reduction of sample matrices (Fig. 6A) and relatively high recoveries (82–94%) for 200 and 500 ppb (Table 2). The recovery for the low concentration (50 ppb) was also acceptable as the concentration range of primary concern for Canadian regulatory agencies is 0.2–10 ppm.[35] The loss of analyte and variation in results could be attributed to the slightly less compact slurry packing of the MIP microspheres on-chip as compared to a manually packed stainless steel HPLC column.[36] In addition, the lower recovery at 50 ppb compared to the higher concentrations might be due to the high affinity of MIPs to zearalenone, which resulted in the retention of a trace amount of the analyte even under the eluting conditions. Nonetheless, the recovery and variation in this study were comparable to those reported for the disposable microfluidic on-chip SPE application.[31] The unique design of

Table 2 Analysis of agri-food samples using μMISPE-MS (n = 3)

Sample	Spiked (ppb)	Recovery	CV
Corn	50	73%	15%
	200	94%	6%
	500	82%	3%
Rice	50	71%	3%
	200	88%	11%
	500	90%	11%

CV: coefficient of variation.

the repackable microcolumn also significantly simplifies the sample clean-up process and reduces the cost of material and labour compared to both the conventional sorbent-reusing protocol and the completely disposable approach (*e.g.*, cartridge, membrane).[34,37,38]

4. Conclusions

This study reported the development of a μMISPE-MS method for rapid detection of a mycotoxin in complex agri-food matrices, highlighting the novel design, fabrication, and optimization of a microfluidic chip that supports repacking of μMISPE and the direct integration with MS. The entire analysis, from sample to answer, was completed within 15 min with full automation in sample clean-up and detection. This method achieved an overall recovery of 71–94% for zearalenone in agri-food samples at concentrations below regulated residue levels. The developed μMISPE-MS method offers a promising alternative to improving sample preparation and analyte separation for immediate mass detection, significantly reducing the time and cost associated with conventional sample preparation and (U)HPLC-based separations. Beyond mycotoxin monitoring in agri-food systems, the μMISPE-MS approach can serve as a template for applications in detecting other chemicals in complex matrices with further advancements in MIP synthesis and system optimization.

Data availability

All the data related to this study have been included in the main body of this manuscript.

Author contributions

MZH proposed the project, performed the experiment and data analysis, and drafted the manuscript. JL contributed to the chip automation part of the experiment. TL helped with the mass spectrometry experiment. DRM secured the research funding for the MS equipment and contributed to manuscript revision. YH co-proposed the project and contributed to the experiment and manuscript revision. XL co-proposed the project, edited the manuscript and secured the research funding.

Conflicts of interest

The authors declare no conflict of interest.

Acknowledgements

This project was financially supported by Fonds de recherche du Québec (FRQNT-B2X) to MZH, Fonds de recherche du Québec (FRQNT-B2X) to JL, Natural Sciences and Engineering Research Council of Canada (RGPIN-2022-04892) to YH, and Natural Sciences and Engineering Research Council of Canada (CRDPJ532306) to XL.

References

1 Agriculture and Agri-Food Canada, *Overview of Canada's agriculture and agri-food sector*, **https://agriculture.canada.ca/en/sector/overview**, (accessed Aug 30, 2024).
2 M. Eskola, G. Kos, C. T. Elliott, J. Hajšlová, S. Mayar and R. Krska, *Crit. Rev. Food Sci. Nutr.*, 2020, **60**, 2773–2789, DOI: **10.1080/10408398.2019.1658570**.
3 M. Tola and B. Kebede, *Cogent Food Agric.*, 2016, **2**, 1191103, DOI: **10.1080/23311932.2016.1191103**.
4 Canadian Food Inspection Agency, *Analytical methods for the determination of nutrients, inorganic and organic compounds and contaminants, and biological contaminants in livestock feeds*, 2022, **https://inspection.canada.ca/animal-health/livestock-feeds/inspection-program/analytical-methods-for-the-determination-of-nutrie/eng/1566313727551/1566313883254**, (accessed Aug 30, 2024).
5 K. Zhang and K. Banerjee, *Toxins*, 2020, **12**, 539, DOI: **10.3390/toxins12090539**.
6 B. Greer, O. Chevallier, B. Quinn, L. M. Botana and C. T. Elliott, *TrAC, Trends Anal. Chem.*, 2021, **141**, 116284, DOI: **10.1016/j.trac.2021.116284**.
7 M. L. Williams, A. A. Olomukoro, R. V. Emmons, N. H. Godage and E. Gionfriddo, *J. Sep. Sci.*, 2023, **46**, 2300571, DOI: **10.1002/jssc.202300571**.
8 D. Steiner, A. Malachová, M. Sulyok and R. Krska, *Anal. Bioanal. Chem.*, 2021, **413**, 25–34, DOI: **10.1007/s00216-020-03015-7**.
9 M. Sulyok, D. Stadler, D. Steiner and R. Krska, *Anal. Bioanal. Chem.*, 2020, **412**, 2607–2620, DOI: **10.1007/s00216-020-02489-9**.
10 D. Steiner, M. Sulyok, A. Malachová, A. Mueller and R. Krska, *J. Chromatogr. A*, 2020, **1629**, 461502, DOI: **10.1016/j.chroma.2020.461502**.
11 L. Campone, A. L. Piccinelli, R. Celano, I. Pagano, M. Russo and L. Rastrelli, *J. Chromatogr. A*, 2016, **1428**, 212–219, DOI: **10.1016/j.chroma.2015.10.094**.
12 S. Rodriguez-Mozaz, M. J. Lopez de Alda and D. Barceló, *J. Chromatogr. A*, 2007, **1152**, 97–115, DOI: **10.1016/j.chroma.2007.01.046**.
13 N. Convery and N. Gadegaard, *Micro Nano Eng.*, 2019, **2**, 76–91, DOI: **10.1016/j.mne.2019.01.003**.
14 S.-M. Yang, S. Lv, W. Zhang and Y. Cui, *Sensors*, 2022, **22**, 1620, DOI: **10.3390/s22041620**.
15 C. M. Leung, P. de Haan, K. Ronaldson-Bouchard, G.-A. Kim, J. Ko, H. S. Rho, Z. Chen, P. Habibovic, N. L. Jeon, S. Takayama, M. L. Shuler, G. Vunjak-Novakovic, O. Frey, E. Verpoorte and Y.-C. Toh, *Nat. Rev. Methods Primers*, 2022, **2**, 33, DOI: **10.1038/s43586-022-00118-6**.
16 X. Liao, Y. Zhang, Q. Zhang, J. Zhou, T. Ding and J. Feng, *Trends Food Sci. Technol.*, 2023, **135**, 115–130, DOI: **10.1016/j.tifs.2023.03.022**.
17 A.-M. Mitrogiannopoulou, V. Tselepi and K. Ellinas, *Micromachines*, 2023, **14**, 986, DOI: **10.3390/mi14050986**.
18 W. Jiang, Q. Tang, Y. Zhu, X. Gu, L. Wu and Y. Qin, *Food Chem.*, 2024, **441**, 138319, DOI: **10.1016/j.foodchem.2023.138319**.

19 Y. Saylan, Ö. Altıntaş and A. Denizli, *Results Opt.*, 2023, **13**, 100541, DOI: **10.1016/j.rio.2023.100541**.
20 M. Z. Hua, S. Li, M. S. Roopesh and X. Lu, *Lab Chip*, 2024, **24**, 2700–2711, DOI: **10.1039/D4LC00193A**.
21 B. Yu, H. Cong, L. Xue, C. Tian, X. Xu, Q. Peng and S. Yang, *Anal. Methods*, 2016, **8**, 919–924, DOI: **10.1039/C5AY02655E**.
22 Y. Zhang, L. Guo, Y. Li, X. He, L. Chen and Y. Zhang, *Sepu*, 2021, **39**, 1137–1145, DOI: **10.3724/SP.J.1123.2021.06024**.
23 R. Gadzała-Kopciuch, K. Kwaśniewska, A. Ludwiczak, P. Skrzyniarz, R. Jakubowski, W. Nowak, A. Wojtczak and B. Buszewski, *Int. J. Mol. Sci.*, 2019, **20**, 1588, DOI: **10.3390/ijms20071588**.
24 J. J. BelBruno, *Chem. Rev.*, 2019, **119**, 94–119, DOI: **10.1021/acs.chemrev.8b00171**.
25 B. Fresco-Cala, A. D. Batista and S. Cárdenas, *Molecules*, 2020, **25**, 4740, DOI: **10.3390/molecules25204740**.
26 A. Gaspar, M. E. Piyasena and F. A. Gomez, *Anal. Chem.*, 2007, **79**, 7906–7909, DOI: **10.1021/ac071106g**.
27 Z. Huang, J. He, Y. Li, C. Wu, L. You, H. Wei, K. Li and S. Zhang, *J. Chromatogr. A*, 2019, **1602**, 11–18, DOI: **10.1016/j.chroma.2019.05.022**.
28 L. Ceriotti, N. F. de Rooij and E. Verpoorte, *Anal. Chem.*, 2002, **74**, 639–647, DOI: **10.1021/ac0109467**.
29 H. Tang, Q. Yu, X. Qian, K. Ni and X. Wang, *Micromachines*, 2018, **9**, 212, DOI: **10.3390/mi9050212**.
30 J. Huft, C. A. Haynes and C. L. Hansen, *Anal. Chem.*, 2013, **85**, 1797–1802, DOI: **10.1021/ac303153a**.
31 J. Chen, F. Liu, Z. Li, L. Tan, M. Zhang and D. Xu, *Microchem. J.*, 2021, **167**, 106298, DOI: **10.1016/j.microc.2021.106298**.
32 G. J. Maranata, N. O. Surya and A. N. Hasanah, *Heliyon*, 2021, **7**, e05934, DOI: **10.1016/j.heliyon.2021.e05934**.
33 J. L. Urraca, M. D. Marazuela, E. R. Merino, G. Orellana and M. C. Moreno-Bondi, *J. Chromatogr. A*, 2006, **1116**, 127–134, DOI: **10.1016/j.chroma.2006.03.032**.
34 AFFINISEP, *Selective solid phase extraction of zearalenone from cereals products, cerealbased foods and babyfood for infants and children using molecularly imprinted polymers*, **https://www.affinisep.com/wp-content/uploads/2021/09/application_note_affinimip_spe_zon_cereal_products_and_baby_food__110429__043781500_1514_01092011.pdf**, (accessed Aug 30, 2024).
35 Canadian Food Inspection Agency, RG-8 Regulatory Guidance: Contaminants in Feed, 2024, **https://inspection.canada.ca/animal-health/livestock-feeds/regulatory-guidance/rg-8/eng/1347383943203/1347384015909?chap=1**, (accessed Aug 30, 2024).
36 J. L. Urraca, M. D. Marazuela and M. C. Moreno-Bondi, *Anal. Bioanal. Chem.*, 2006, **385**, 1155–1161, DOI: **10.1007/s00216-006-0343-3**.
37 T. Sergeyeva, D. Yarynka, L. Dubey, I. Dubey, E. Piletska, R. Linnik, M. Antonyuk, T. Ternovska, O. Brovko, S. Piletsky and A. El'skaya, *Sensors*, 2020, **20**, 4304, DOI: **10.3390/s20154304**.
38 Y. Zhang, J. He, L. Song, H. Wang, Z. Huang, Q. Sun, X. Ba, Y. Li, L. You and S. Zhang, *Anal. Bioanal. Chem.*, 2020, **412**, 4045–4055, DOI: **10.1007/s00216-020-02610-y**.